BMSC-derived Exosomes Protect Against Delayed Encephalopathy after Acute Carbon Monoxide Poisoning in Rats via Blockade of Notch Signaling

Xiang Yan
Affiliated Hospital of Southwest Medical University
Meng Fu
Affiliated Hospital of Southwest Medical University
Ye Gao
Affiliated Hospital of Southwest Medical University
Qin Han
Affiliated Hospital of Southwest Medical University
Shuang Li
Affiliated Hospital of Southwest Medical University
Huan Xia
Affiliated Hospital of Southwest Medical University
Jinglun Li (ljl0310611@163.com)
Affiliated Hospital of Southwest Medical University

Research Article

Keywords: DEACMP, exosome, Notch, Treg, cognitive impairment, immunomodulation

Posted Date: October 21st, 2021

DOI: https://doi.org/10.21203/rs.3.rs-879944/v1

Abstract

Objective: Our aim was to probe the therapeutic effect by which (BMSC-ex) protect against (DEACMP) in rat models in vivo.

Methods: BMSC-ex were successfully characterized and proven to pass the blood brain barrier and migrate to the injured brain area. Rats were randomly divided into six groups and the cognitive function of mice was evaluated by the morris water maze. The severity of pathological changes was evaluated by HE staining and LFB staining. The expression of cytokines was detected by ELISA. Immunohistochemical staining and western blot analysis were utilized to detect the protein expression of Foxp3、CD4、MBP、Notch1 and Hess1 in brain tissue.

Results: We found that BMSC-ex significantly reduced inflammation, increased the levels of (Tregs), relieved demyelination, and ameliorated the cognitive impairment in DEACMP rats. Furthermore, inhibiting the Notch pathway led to a partial reversal of the effect of BMSC-ex in mice.

Conclusions: BMSC-ex relieved the severity of demyelination in the DEACMP rat models by regulating Tregs subsets and the expression of Notch signaling. Hence BMSC-ex play a protected role in DEACMP by upregulating Tregs and the regulatory components of Notch signaling and this may provide a new clinical strategy for the treatment of DEACMP patients.

1. Introduction

Delayed encephalopathy after acute carbon monoxide poisoning (DEACMP) occurs in about 2-30% patients during the relapse of neuropsychiatric symptoms after a 2-40 days period of remission, called the “lucid interval”, following the symptoms of acute carbon monoxide poisoning symptoms[1][2][3]. The clinical manifestations of DEACMP are characterized by a subacute course of cognitive impairment with varying severity, such as parkinsonism, incontinence, dementia, and psychosis[4][5][6]. However, its molecular biological mechanisms remain unclear. The pathological mechanism of DEACMP is hypothesized to include the involvement of myelin basic protein (MBP)-mediated autoimmune cascade reaction, followed by the slow progressive accumulation of demyelinating events[7].

BMSC-derived exosomes are nano-sized extracellular vesicles loaded with various RNAs and proteins, and act as paracrine factors in intercellular communication[8][9]. Exosome-based therapy is an emerging modality in various inflammatory conditions involving an overactive immune system[10][11], and has shown promising effects in clinical trials and experimental models[12]. Several studies have demonstrated that the modulation of regulatory T cells (Tregs) is due to immunoregulatory effects of exosomes[13][14]. However, the application of exosomes in a rat model of DEACMP has not been addressed.

Thus, we investigated the therapeutic potential of BMSC-derived exosomes on DEACMP and analyzed the underlying Notch signaling pathway.

2. Materials And Methods

2.1 Animals and experimental design

Male Sprague-Dawley (SD) rats weighting 200-250 g were obtained from the Experimental Animal Center of Southwest Medical University and placed in a thermostatic specific pathogen-free laboratory animal room with free access to feeds and water. In this experiment, all animals were starved for one week prior to the experimental work, then randomly divided into six groups (n=10): NC, CO, BMSC-ex, GW4869, DAPT, and BMSC-ex +DAPT group. DEACMP models were induced as previously described. Briefly rats excluding the NC group were exposed to CO (1,000 ppm) for 40 min followed by a second exposure to CO (3,000 ppm) for 20 min in a hyperbaric oxygen chamber[15]. Rats in the BMSC-ex, GW4869, and BMSC-ex + DAPT groups were injected with exosomes (100 μg/mouse) by the tail vein 1 h after DEACMP induction[12]. Next, GW4869 (2.5μg/g, Sigma, USA) was diluted in dimethyl sulfoxide and intraperitoneally administered in the GW4869 group[16]. The DAPT was applied to the DAPT and BMSC-ex +DAPT group at doses of 1 mg /kg[17]. Fourteen days post-CO exposure, rats were sacrificed for brain tissue collection under deep anesthesia by 10% pentobarbital sodium (40 mg/kg)[18].

2.2 Isolation and culture of BMSCs

Isolation and culturing of BMSCs was performed as previously reported protocol[19]. The rats were anesthetized using pentobarbital and immersed in ethanol (70%) for disinfection. The femurs and tibia of rats were removed from tissues. Bones were sterilized in a tube with 70% ethyl alcohol for 2 min and then steeped in phosphate-buffered saline (PBS) for 30 min under ultraviolet disinfection. The marrow cavity is exposed by cutting off the epiphysis at each end of the bone. A syringe was used to draw the cell growth fluid, with the needle was alternately inserted into their ends to rinse, until the marrow cavity turned white. The cell growth fluid consisted of Dulbecco's modified Eagle medium (90%; Gibco, USA), fetal bovine serum (10%; HYCLONE, USA), PEN-STREP (1%; Lonza, USA) and L-VC (1%). Collected samples were placed in 60 mm culture dishes and routinely cultured in a 5% CO_2 incubator at 37 ° C. After 48 h, half of the cell growth fluid was discarded and the medium was replaced completely every three days. BMSCs at approximately 80% confluency were subcultured.

2.3 Extraction and identification of exosomes

The BMSCs culture supernatant was collected to extract exosomes by ultracentrifugation as described previously[20]. After incubating BMSCs for 72 h in an exosome-depleted medium to avoid the interference of exosomes from media, the spent medium was collected and alternately centrifuged at low and high speeds. Centrifugation was carried out at 300 x g for 10 min to remove cells, and then at 2000 × g for 10 min to remove dead cells. The supernatant was centrifuged at 100,000 x g for 30 min to discard cells debris and centrifuged again at 100,000 x g for 70 min to discard the supernatant. The pellet was washed in PBS and recentrifuged at 100,000 x g for 70 min. Finally, the pellet was resuspended in PBS and stored

at -80 ℃. Further procedures were carried out at 4 ℃ to authenticate exosomes at three levels: surface markers authenticated by western blot, morphology visualized by transmission electron microscopy, and size by nanoparticle tracking analysis.

2.4 Morris water maze test

The cognitive impairment of the rats was evaluated by the Morris water maze test as reported earlier[21]. In order to adapt to the new environment, the rats were put into the water to swim for 2 min before the formal training. In the place navigation test, rats were placed into each of four quadrants toward the wall of the pool under water, and the time required for the rats to find the underwater platform and stand on it was recorded as escape latency. If the rats could not find the platform after 2 min, they were pulled onto the platform and the time was recorded as 120 s. When the rats learned to find the platform, we removed the platform and placed rats into water from the same position. The number of times of crossing the platform was recorded.

2.5 Luxol fast blue (LFB)

Paraffin slices of brain tissue were sequentially immersed in toluene for 20 min, toluene - anhydrous alcohol for 20 min, anhydrous alcohol for 10 min, 95% alcohol for 5 min, 90% alcohol for 5 minutes, 80% alcohol for 5 min, and 70% alcohol for 5 min. The processed sections were incubated overnight in 0.1% LFB solution, and successively immersed in 95% HCl and 70% ethanol until white matter stained blue and gray matter appeared colorless.

2.6 Enzyme-linked immunosorbent assay

Brain tissues were centrifuged at 5000 x g for 10 min, and the supernatant retained. Rat tumor necrosis factor (TNF)-α, interferon (IFN)-γ, interleukin (IL)-10 and tumor necrosis factor (TGF)-β kits (eBioscience, USA) were used to estimated cytokine levels according to the manufacturer's instruction. A microplate reader (Biotek, USA) was used to measure the absorbance at 450 nm; the data obtained were analyzed using the Gen5 software.

2.7 Immunofluorescence analysis

Paraffin slices of the brain tissue were dewaxed with water in a 65 ℃ oven for 2h and were washed with PBS. The non-specific binding sites were blocked with 5% BSA for 20 min. After removing the BSA solution, primary antibodies for anti-Foxp3 (1:50; Ab22510; Abcam, USA), anti-CD4 (1:50; A0362; Abclonal, Wuhan, China), anti-MBP (1:200; BA0094; Boster, USA), anti-Notch1 (1:150; 10062-2-Ap, Ptg) were added accordingly to each section and incubated overnight at 4 ℃. After washing thrice with PBS, sections were incubated with a secondary antibody, such as goat-anti-rabbit (1:50; AS-1110; Aspen, USA)

or goat-anti-mouse (1:50; AS-1112; Aspen, USA) at 37 ℃ for 50 min. Sections were incubated with 50-100μL DAPI solution (1:1000, AS1075; Aspen, USA) at room temperature for 5 min, in darkness. An appropriate amount of anti-fluorescence quenching agent was added to the tissue, the cover glass sealed, and observed under a fluorescence microscope.

2.8 Western blotting analysis

Proteins samples were separated by 12% SDS-PAGE (AS1012; ASPEN, USA) from exosomes or brain tissues, then transferred onto polyvinylidene difluoride membranes (IPVH00010; Millipore, USA) and blocked with TBST for 1 h. Primary antibodies foe anti-CD9 (1:1000; bs23032R; BIOSS, USA), CD63 (1:1000; Ab109201; Abcam, USA), anti-TSG101 (1:1000, 14497-1-AP), anti-GAPDH (1:10000; Ab37168; Abcam, USA), anti-Foxp3 (1:1000; Ab215206; Abcam, USA), anti-CD4 (1:1000, 19068-1-AP), anti-MBP (1:1000; Ab11159; Abcam, USA), anti-Notch1 (1:500; sc-376403; Santa, USA), and anti-Hess-1 (1:10000; Ab108937; Abcam, USA) were added to the membranes and incubated together overnight at 4°C. After washing thrice with TBST, secondary antibodies (all diluted 1:10000; ASPEN, AS1106 for mouse-antibody and AS1107 for rabbit-antibody) were added and incubated at room temperature for 1 h. Finally, the band was detected by chemiluminescence and the intensity was analyzed by ImageJ software.

2.9 Statistical analysis

GraphPad Prism v 7.01. was used for all statistical analyses in this experiment. Data was analyzed using one-way or two-way repeated measures analysis of variance with post-hoc Tukey's multiple comparisons. All data presented as mean ± SEM (n=3) were statistically significant when $P < 0.05$.

3. Results

3.1 Characterization of BMSC-derived exosomes

Before the injection of exosomes, the characteristics of exosomes derived from BMSCs were identified. As shown in Figure 1A, extracellular vesicles in this study showed symbolic molecular markers typical of exosomes secreted from BMSCs, with positive expressions of CD9, CD63 and TSG101, by western blotting. BMSC-ex was visualized as an irregular ellipse with an obvious bi-layer membrane structure under transmission electron microscopy (Figure 1B). Results of nanoparticle tracking analysis showed that BMSC-ex size distribution ranged from 30 to 150 nm (Figures 1C). Altogether, these results were consistent with previously documented descriptions of exosomes secreted from BMSCs[22][23], thus indicating the successful isolation of BMSCs-ex.

To confirm whether BMSC-ex could traverse the blood-brain barrier, we labeled BMSC-ex with Phalloidin, a known stain for CT imaging in vivo. Phalloidin-loaded BMSC-ex were administered 1 h after acute CO poisoning. As shown in Figure 1D-E, a substantial amount of phalloidin was accumulated in the brain

and liver 24 h after administration (Figure 1E), compared with that before administration (Figure 1D). The qualitative micro-CT scan demonstrated that BMSC-ex could effectively penetrate the blood-brain barrier and reach the areas of lesion.

3.2 BMSC-derived exosomes alleviated cognitive impairment induced by CO exposure.

BMSC-ex injections promoted spatial learning and spatial memory on the Morris water maze test. Both the prolonged escape latency and reduced times of crossing the platform for the CO group demonstrated significant cognitive impairment 14 days post-CO exposure compared with NC group ($P < 0.05$) (Figure2A, B). When compared to the CO group, the BMSC-ex group showed a significant decrease in the escape latency from the 14th day to the 21th day ($P < 0.05$) and significantly increased times of crossing the platform from the 21th day to the 28th day ($P <0 .05$) (Figure 2B). However, after effectively inhibiting the secretion of exosomes by GW4869[24], an established inhibitor, both spatial learning and spatial memory did not exhibit a noticeable difference between the CO group and BMSC-ex+GW4869 group ($P > 0.05$) (Figure2A, B).

3.3 BMSC-derived exosomes improved the proliferation of Tregs in DEACMP rats

The WB expression of Foxp3 and CD4 (Figure 3A-C) indicated a lower expression in the brain of the CO group compared with the NC group ($P<0.05$). In contrast, higher Foxp3 and CD4 levels were observed in the BMSC-ex group($P<0.05$) (Figure 3A-C), although still lower than in the NC group. The protein levels of Foxp3 and CD4 were not significantly different between the CO group and the BMSC-ex+GW4869 group. Immunofluorescent staining exhibited similar results as above (Figure 3D). Altogether these data suggested that BMSC-ex dramatically promote the proliferation of Tregs in a rat model of DEACMP.

3.4 BMSC-derived exosomes alleviated inflammatory responses induced by CO exposure.

To further probe the status of neuroimmune responses post-CO exposure, we determined the concentrations of inflammatory cytokines relevant to DEACMP two weeks after being poisoned. The levels of both TNF-α and IFN-γ remarkably increased after CO exposure ($P < 0.05$) (Figure 4A-B). On the contrary, the levels of TGF-β and IL-10 were significantly decreased ($P<0.05$) at this point (Figure 4C, D). BMSC-ex partly reversed the CO-induced increase of pro-inflammatory factors, TNF-α and IFN-γ, and the reduction of anti-inflammatory factors, TGF-β and IL-10($P<0.05$) (Figure 4A-D). The aforementioned inflammatory cytokines in the BMSC-ex + GW4869 group were similar to those of the CO group($P>0.05$) (Figure 4).

3.5 BMSC-derived exosomes alleviated damage of myelin in the white matter of brain.

The extent of damage of myelin was assessed by LFB staining, and the protein levels of MBP in the brain. Fourteen days after CO poisoning, the LFB staining demonstrated that the dark blue-stained stripe significantly decreased, clearly broke and became shorter in the CO group (Figure. 5A). Furthermore, the lower protein levels of MBP in the CO group also indicated that CO-poisoning could cause sharp MBP degradation and severe demyelination in the brain tissues ($P< 0.05$) (Figure. 5B-D). When treated with exosomes, rats in the BMSC-ex group substantially promoted the remodeling of myelin sheath and alleviated impairment of MBP ($P< 0.05$) (Figure. 5A-D). Additionally, the absence of an improvement in demyelination upon the addition of the exosome inhibitor (BMSC-ex +GW4869 group) suggested that BMSC-ex relieved the damage of myelin and enhanced remyelination.

3.6 DAPT partly reversed the effect of BMSC-derived exosomes on the proliferation of Tregs.

To corroborate the underlying mechanism of BMSC-ex on the Tregs in the brain, the WB and immunofluorescent staining were analyzed after inhibiting Notch signaling using a γ-secretase inhibitor, DAPT[25]. Western blotting analysis showed that the protein levels of Notch1 and Hess1 were notably decreased in the DAPT-treated rats ($P<0.05$), thereby suggesting that DAPT effectively inhibited the Notch signaling pathway (Figure6A, B). Additionally, the proliferation capability of Tregs and the protein level of MBP was steeply reduced in the rats treated with DAPT, and the protein levels of Foxp3, CD4, and MBP were lower in the DAPT group than those in the BMSC-ex +DAPT group (Figure 6C-G) ($P<0.05$). Thus, the blockade of the Notch signaling pathway partly reversed the therapeutic effect of BMSC-ex in the rats model of DEACMP.

4. Discussion

In our study, we aimed to probe the immunoregulatory potential of exosomes in DEACMP rat model. At present, experiments focused on the application of immunoregulatory effect of exosomes to DEACMP are scant, and this is a preliminary attempt to explore it.

Gross anatomical analysis of the brains from rats subjected to CO poisoning have previously revealed numerous neuropathological abnormalities in the white matter[26]. The critical mechanism of DEACMP is hypothesized to involve a MBP-mediated autoimmune cascade: MBP undergoes lipid peroxidation after CO poisoning and loses its normal characteristics, thereby resulting in successive recognition by an antibody to activate the adaptive immunological response[27][28]. When the progressing injuries of MBP exceed an unknown tripping point, pathophysiological variations in brain tissues and a succession of neurodegenerative symptoms could occur in some patients. Researchers have further demonstrated that rats immunologically tolerant to MBP showed biochemical changes in MBP, but no lymphocyte

proliferative response or cognitive decline. Numerous publications have shown that the injection of exosomes could improve recognitive deficits in autoimmune and neurodegenerative diseases[13]. Studies have demonstrated that the sensorimotor function of rats after traumatic brain injury is significantly enhanced by the administration of BMSC-derived exosomes[29]. Research focusing on the experimental autoimmune uveoretinitis illustrated that MSC-secreted exosomes reduced excitation as well as aggregation of leukocytes, and attenuated inflammation response[30]. BMSC-ex are known to alleviate symptoms of several autoimmune and cognitive disorders, and therefore possess therapeutic potential in DEACMP.

In the present study, we confirmed that BMSC-ex dramatically relieved cognitive decrement and enhanced remyelination as well as the expression of MBP, a component as one of the most indispensable components of the myelin[31]. We also demonstrated that BMSC-ex could upregulated the Tregs and suppress the inflammatory response in the rat model. The protein levels of CD4 and Foxp3, regarded as biomarkers of Tregs, declined prominently due to DEACMP, while a notably moderate trend was observed after BMSC-ex treatment. Previous studies have reported that Tregs exerted substantial immunosuppressive effects and mediated immune tolerance, which are regulated by the expression of Foxp3[32][33]. Thus, our results suggested that Tregs may be activated and recruited into the brain lesions after treatment by BMSC-ex in DEACMP rats, which is in accordance with studies observing a surge in the number of Tregs[13][34]. Additionally, our study follows the changes in the inflammatory cytokines in brain tissues, thereby revealing anti-inflammatory action of exosomes. That is similar to the pathophysiological process of some neuroimmune disorders[34][35][36]. In some autoimmune disorders, TGF-β, a promoting and secreting factor of Tregs, together with IL-10 mediates immunosuppressive functions and inhibits inflammatory factors IFN-γ and TNF-α[37]. In summary, our results demonstrated that excessive neuroimmune responses as a results of CO poisoning were mitigated by BMSC-ex treatment via modulating expression of Tregs.

The Notch signaling pathway is a vital regulator of immune cells and inflammatory reactions, and closely engages in a variety of autoimmune diseases[38]. Meanwhile, Notch has been reported to exert a positive effect on the differentiation of Tregs[39][40]. In the present study, the fluctuation in Notch-1 and Hess-1 levels suggested that the blockade of the Notch signaling pathway by its inhibitor, DAPT, partially reversed the immunosuppressive function and therapeutic effect of BMSC-ex. Thus, we speculate that BMSC-ex ameliorated DEACMP via inhibiting the Notch signaling pathway; however further investigations are needed to confirm this hypothesis.

Some limitations in our study should be noted. First, in the absence of supporting research on the cellular models of DEACMP, we were unable to investigate the effect of BMSC-ex on DEACMP in vitro. Second, exosomes as extracellular vesicles carry diverse microRNAs, proteins, and lipids, but we did not focus on their specific component. This drives us to further explore the specific molecular components involved in the therapeutic mechanism of exosomes.

5. Conclusion

Our results demonstrate that exosomes secreted from BMSCs could attenuate CO-induced damage to myelin and cognitive impairment via Notch-mediated upregulation of Tregs and thereby alleviated of neuroinflammation. Our findings may bring new prospects for the treatment of DEACMP.

Abbreviations

DEACMP: delayed encephalopathy after acute carbon monoxide poisoning;

BMSC: bone marrow mesenchymal stem cells;

BMSC-ex: BMSC-derived exosomes;

Tregs: regulatory T cells;

ELISA: enzyme linked immunosorbent assay;

LFB: luxol fast blue;

IF: Immunofluorescence;

TNF-α: rat tumor necrosis factor-α;

IFN-γ: interferon-γ;

IL-10: interleukin-10;

TGF-β: tumor necrosis factor-β.

Declarations

Ethics approval and consent to participate

Animal procedures were conducted in accordance with the guidelines of the European Directive 2010/63/EU and was approved by the Ethics Committee of Southwest Medical University (Approval No.20210006). This study was carried out in compliance with ARRIVE guidelines.

Consent for publication

Not applicable.

Availability of data and materials

All data generated or analysed during the current study are included in this published article. Futher data will be shared by request from corresponding author on reasonable request.

Competing interests

The authors declare that they have no competing interest.

Funding

This study was financially supported by the Luzhou People's Government-Southwest Medical University science and technology strategic cooperation project (Grant No.2017LZXNYD-J36).

Authors' contributions

YX and LJ designed the work, and wrote the manuscript. YX, FM, LS, XH, GY, and HQ assisted to performed the experiments and analyzed the data. All authors have reviewed and approved the final version of the manuscript, and agree to be accountable for all aspects of the work.

References

1. Guo D, Hu H, Pan S. Oligodendrocyte dysfunction and regeneration failure: A novel hypothesis of delayed encephalopathy after carbon monoxide poisoning. Med Hypotheses. 2020;136:109522. doi:10.1016/j.mehy.2019.109522.
2. Weaver LK, Valentine KJ, Hopkins RO. Carbon monoxide poisoning: Risk factors for cognitive sequelae and the role of hyperbaric oxygen. Am J Respir Crit Care Med. 2007;176:491–7.
3. Yıldırım Z, Altunkaynak Y, Baybaş S. Delayed encephalopathy after carbon monoxide intoxication: case report. Acta Neurol Belg. 2020;120:1213–4. doi:10.1007/s13760-019-01222-3.
4. Huang CC, Ho CH, Chen YC, Hsu CC, Lin HJ, Wang JJ, et al. Autoimmune connective tissue disease following carbon monoxide poisoning: A nationwide population-based cohort study. Clin Epidemiol. 2020;12:1287–98.
5. Huang CC, Chung MH, Weng SF, Chien CC, Lin SJ, Lin HJ, et al. Long-term prognosis of patients with carbon monoxide poisoning: A nationwide cohort study. PLoS One. 2014;9.
6. Zou JF, Guo Q, Shao H, Li B, Du Y, Liu M, et al. Lack of pupil reflex and loss of consciousness predict 30-day neurological sequelae in patients with carbon monoxide poisoning. PLoS One. 2015;10:1–9.
7. Thom SR, Bhopale VM, Han ST, Clark JM, Hardy KR. Intravascular neutrophil activation due to carbon monoxide poisoning. Am J Respir Crit Care Med. 2006;174:1239–48.
8. Wang J, Hendrix A, Hernot S, Lemaire M, De Bruyne E, Van Valckenborgh E, et al. Bone marrow stromal cell-derived exosomes as communicators in drug resistance in multiple myeloma cells.

Blood. 2014;124:555–66.

9. Yang D, Zhang W, Zhang H, Zhang F, Chen L, Ma L, et al. Progress, opportunity, and perspective on exosome isolation - Efforts for efficient exosome-based theranostics. Theranostics. 2020;10:3684–707.
10. Février B, Raposo G. Exosomes: Endosomal-derived vesicles shipping extracellular messages. Curr Opin Cell Biol. 2004;16:415–21.
11. Guo CH, Han LX, Wan MR, Deng GJ, Gan JH. Immunomodulatory effect of bone marrow mesenchymal stem cells on T lymphocytes in patients with decompensated liver cirrhosis. Genet Mol Res. 2015;14:7039–46.
12. Li Z, Liu F, He X, Yang X, Shan F, Feng J. Exosomes derived from mesenchymal stem cells attenuate inflammation and demyelination of the central nervous system in EAE rats by regulating the polarization of microglia. Int Immunopharmacol. 2019;67 September 2018:268–80. doi:10.1016/j.intimp.2018.12.001.
13. Riazifar M, Mohammadi MR, Pone EJ, Yeri A, Lasser C, Segaliny AI, et al. Stem Cell-Derived Exosomes as Nanotherapeutics for Autoimmune and Neurodegenerative Disorders. ACS Nano. 2019;13:6670–88.
14. Wang G-J, Liu Y, Qin A, Shah S V., Deng Z, Xiang X, et al. Thymus Exosomes-Like Particles Induce Regulatory T Cells. J Immunol. 2008;181:5242–8.
15. Li Q, Cheng Y, Bi MJ, Lin H, Chen Y, Zou Y, et al. Effects of N-butylphthalide on the activation of Keap1/Nrf-2 signal pathway in rats after carbon monoxide poisoning. Environ Toxicol Pharmacol. 2015;40:22–9. doi:10.1016/j.etap.2015.05.009.
16. Essandoh K, Yang L, Wang X, Huang W, Qin D, Hao J, et al. Blockade of exosome generation with GW4869 dampens the sepsis-induced inflammation and cardiac dysfunction. Biochim Biophys Acta - Mol Basis Dis. 2015;1852:2362–71. doi:10.1016/j.bbadis.2015.08.010.
17. Hao Y, Wang X, Zhang F, Wang M, Wang Y, Wang H, et al. Inhibition of notch enhances the anti-atherosclerotic effects of LXR agonists while reducing fatty liver development in ApoE-deficient mice. Toxicol Appl Pharmacol. 2020;406 June:115211. doi:10.1016/j.taap.2020.115211.
18. Xue NY, Ge DY, Dong RJ, Kim HH, Ren XJ, Tu Y. Effect of electroacupuncture on glial fibrillary acidic protein and nerve growth factor in the hippocampus of rats with hyperlipidemia and middle cerebral artery thrombus. Neural Regen Res. 2021;16:137–42.
19. Liu W, Wang Y, Gong F, Rong Y, Luo Y, Tang P, et al. Exosomes derived from bone mesenchymal stem cells repair traumatic spinal cord injury by suppressing the activation of a1 neurotoxic reactive astrocytes. J Neurotrauma. 2019;36:469–84.
20. Wang J, Yao Y, Wu J, Li G. Identification and analysis of exosomes secreted from macrophages extracted by different methods. Int J Clin Exp Pathol. 2015;8:6135–42.
21. Sadegh M, Fathollahi Y, Naghdi N, Semnanian S. Morphine deteriorates spatial memory in sodium salicylate treated rats. Eur J Pharmacol. 2013;704:1–6. doi:10.1016/j.ejphar.2013.02.017.

22. Luo Z, Lin J, Sun Y, Wang C, Chen J. Bone Marrow Stromal Cell-Derived Exosomes Promote Muscle Healing Following Contusion Through Macrophage Polarization. 2021.
23. Xu YC, Lin YS, Zhang L, Lu Y, Sun YL, Fang ZG, et al. MicroRNAs of bone marrow mesenchymal stem cell-derived exosomes regulate acute myeloid leukemia cell proliferation and apoptosis. Chin Med J (Engl). 2020;133:2829–39.
24. Kosaka N, Iguchi H, Yoshioka Y, Takeshita F, Matsuki Y, Ochiya T. Secretory mechanisms and intercellular transfer of microRNAs in living cells. J Biol Chem. 2010;285:17442–52.
25. Bai XC, Rajendra E, Yang G, Shi Y, Scheres SHW. Sampling the conformational space of the catalytic subunit of human g-secretase. Elife. 2015;4:1–19.
26. Chou MC, Li JY, Lai PH. Longitudinal white matter changes following carbon monoxide poisoning: A 9-month follow-up voxelwise diffusional kurtosis imaging study. Am J Neuroradiol. 2019;40:478–82.
27. Thom SR, Bhopale VM, Fisher D, Zhang J, Gimotty P. Delayed neuropathology after carbon monoxide poisoning is immune-mediated. Proc Natl Acad Sci U S A. 2004;101:13660–5.
28. Thom SR, Bhopale VM, Fisher D. Hyperbaric oxygen reduces delayed immune-mediated neuropathology in experimental carbon monoxide toxicity. Toxicol Appl Pharmacol. 2006;213:152–9.
29. Zhang Y, Chopp M, Zhang ZG, Katakowski M, Xin H, Qu C, et al. Systemic administration of cell-free exosomes generated by human bone marrow derived mesenchymal stem cells cultured under 2D and 3D conditions improves functional recovery in rats after traumatic brain injury. Neurochem Int. 2017;111:69–81. doi:10.1016/j.neuint.2016.08.003.
30. Bai L, Shao H, Wang H, Zhang Z, Su C, Dong L, et al. Effects of Mesenchymal Stem Cell-Derived Exosomes on Experimental Autoimmune Uveitis. Sci Rep. 2017;7:1–11.
31. Kuhlmann T, Ludwin S, Prat A, Antel J, Brück W, Lassmann H. An updated histological classification system for multiple sclerosis lesions. Acta Neuropathol. 2017;133:13–24.
32. Romano M, Fanelli G, Albany CJ, Giganti G, Lombardi G. Past, present, and future of regulatory T cell therapy in transplantation and autoimmunity. Front Immunol. 2019;10 JAN.
33. Zemmour D, Zilionis R, Kiner E, Klein AM, Mathis D, Benoist C. Single-cell gene expression reveals a landscape of regulatory T cell phenotypes shaped by the TCR article. Nat Immunol. 2018;19:291–301. doi:10.1038/s41590-018-0051-0.
34. Seger J, Zorzella-Pezavento SFG, Pelizon AC, Martins DR, Domingues A, Sartori A. Decreased production of TNF-alpha by lymph node cells indicates experimental autoimmune encephalomyelitis remission in Lewis rats. Mem Inst Oswaldo Cruz. 2010;105:263–8.
35. Suryanarayanan A, Carter JM, Landin JD, Morrow AL, Werner DF, Spigelman I. Role of interleukin-10 (IL-10) in regulation of GABAergic transmission and acute response to ethanol. Neuropharmacology. 2016;107:181–8. doi:10.1016/j.neuropharm.2016.03.027.
36. Walter TJ, Crews FT. Microglial depletion alters the brain neuroimmune response to acute binge ethanol withdrawal. J Neuroinflammation. 2017;14:1–19.

37. Qiu R, Zhou L, Ma Y, Zhou L, Liang T, Shi L, et al. Regulatory T Cell Plasticity and Stability and Autoimmune Diseases. Clin Rev Allergy Immunol. 2020;58:52–70.
38. Clara JA, Monge C, Yang Y, Takebe N. Targeting signalling pathways and the immune microenvironment of cancer stem cells — a clinical update. Nat Rev Clin Oncol. 2020;17:204–32. doi:10.1038/s41571-019-0293-2.
39. Magee CN, Murakami N, Borges TJ, Shimizu T, Safa K, Ohori S, et al. Notch-1 Inhibition Promotes Immune Regulation in Transplantation Via Regulatory T Cell-Dependent Mechanisms. 2019.
40. Xu S, Kong YG, Jiao WE, Yang R, Qiao YL, Xu Y, et al. Tangeretin promotes regulatory T cell differentiation by inhibiting Notch1/Jagged1 signaling in allergic rhinitis. Int Immunopharmacol. 2019;72 March:402–12.

Figures

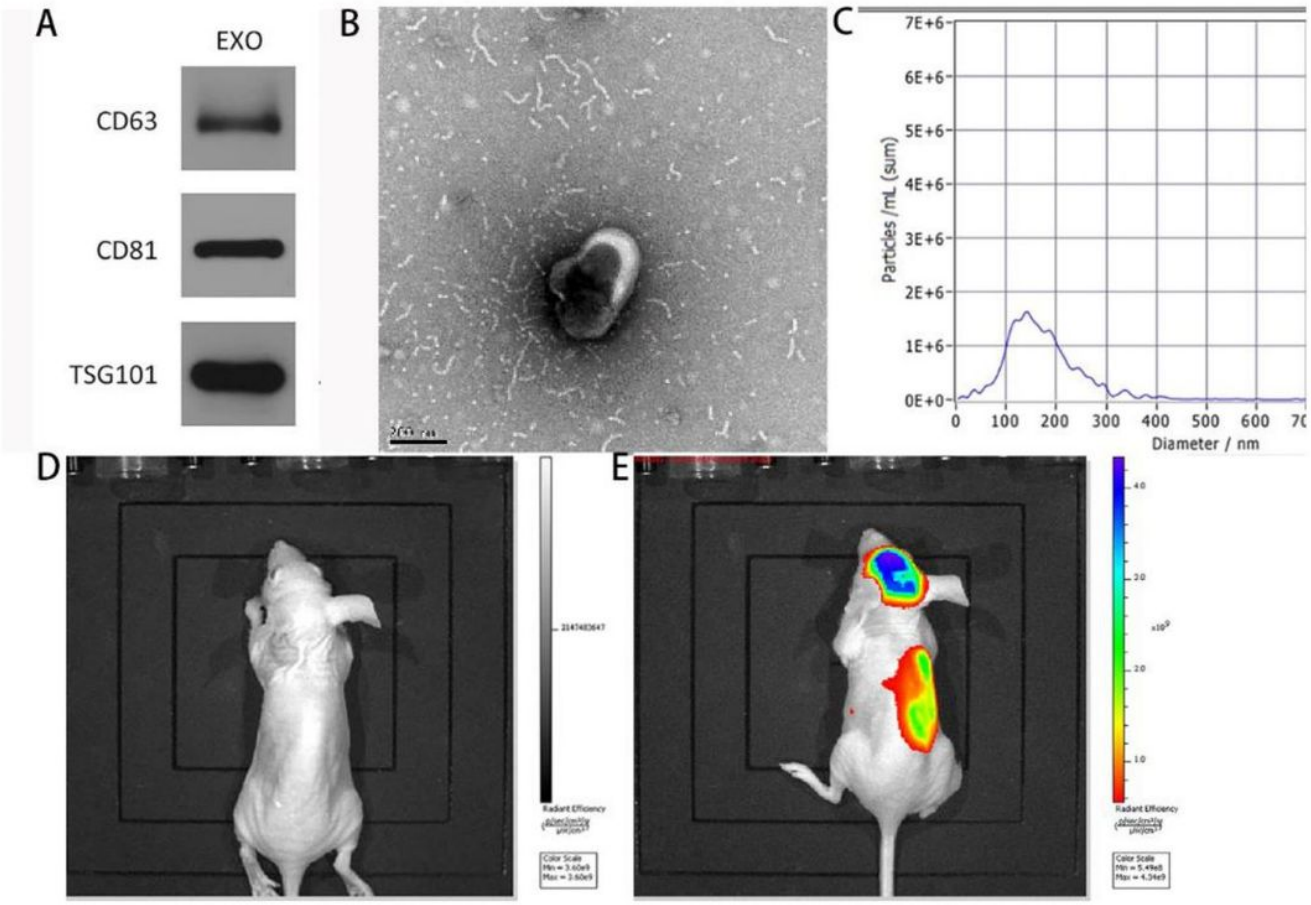

Figure 1

Authentication of exosomes generated from BMSCs and Attesting that BMSC-derived exosomes can penetrate the Blood brain barrier. (A) Western Blot was utilized for detecting CD63, CD81 and TSG101. The full-length blots gels images are presented in Supplementary FigureS1. Representative transmission electron microscopy (B) micrographs of BMSCs-ex. (C) Size profile of BMSC-ex was analyzed by nanoparticle tracking analysis. Images of micro-CT before the injection (D) of exosomes and after the injection(E). Results are representative of three independent experiments.

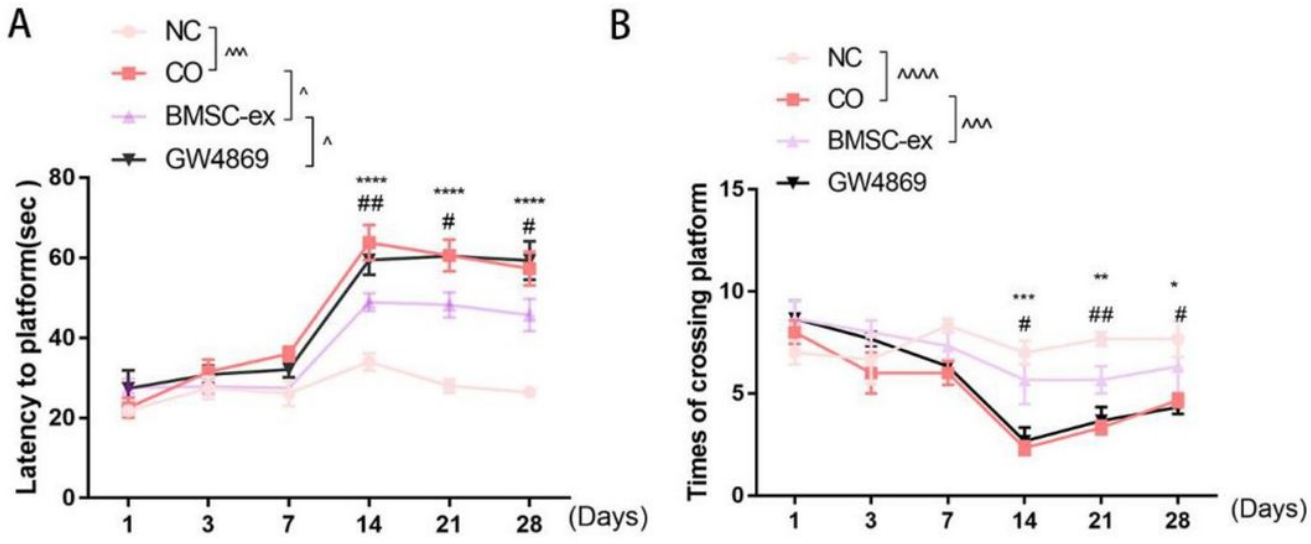

Figure 2

BMSC-derived exosomes alleviated cognitive impairment Induced by CO exposure by the morris water maze test. (A) The place navigation test was conducted to calculate escape latency. (B) The space probe trial test was performed to count the number of times crossing the platform. (*P < 0.05, **P < 0.01, ***P < 0.001, ****P < 0.0001 vs.NC group; #P < 0.05, ##P < 0.01, vs.CO group; ^P< 0.05, ^^P< 0.01, ^^^P< 0.001, ^^^^P< 0.0001).

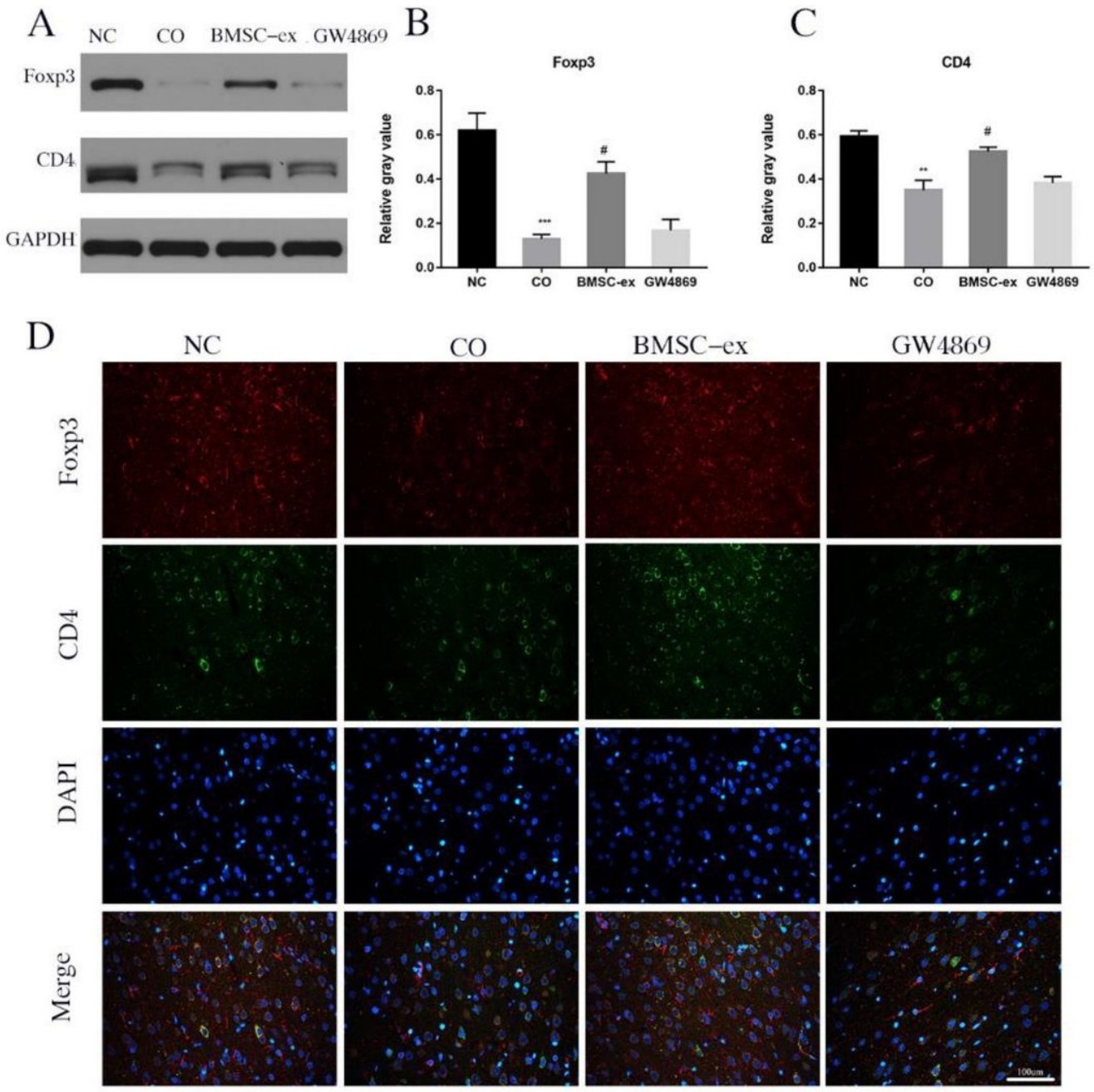

Figure 3

BMSC-derived exosomes improved the upregulation of Tregs in brain tissues of DEACMP rats. (A) Western Blot and (B-C) quantifications were performed to evaluated relative protein expression of Foxp3 and CD4 and normalized protein expression by GAPDH. The full-length blots gels images are presented in Supplementary FigureS2. (D) Immunofluorescence images exhibited expression of Foxp3, CD4 and nuclear in the subcortical. (* P < .05, **P < .01, ***P < .001 vs.NC group; #P < 0.05 vs.CO group)

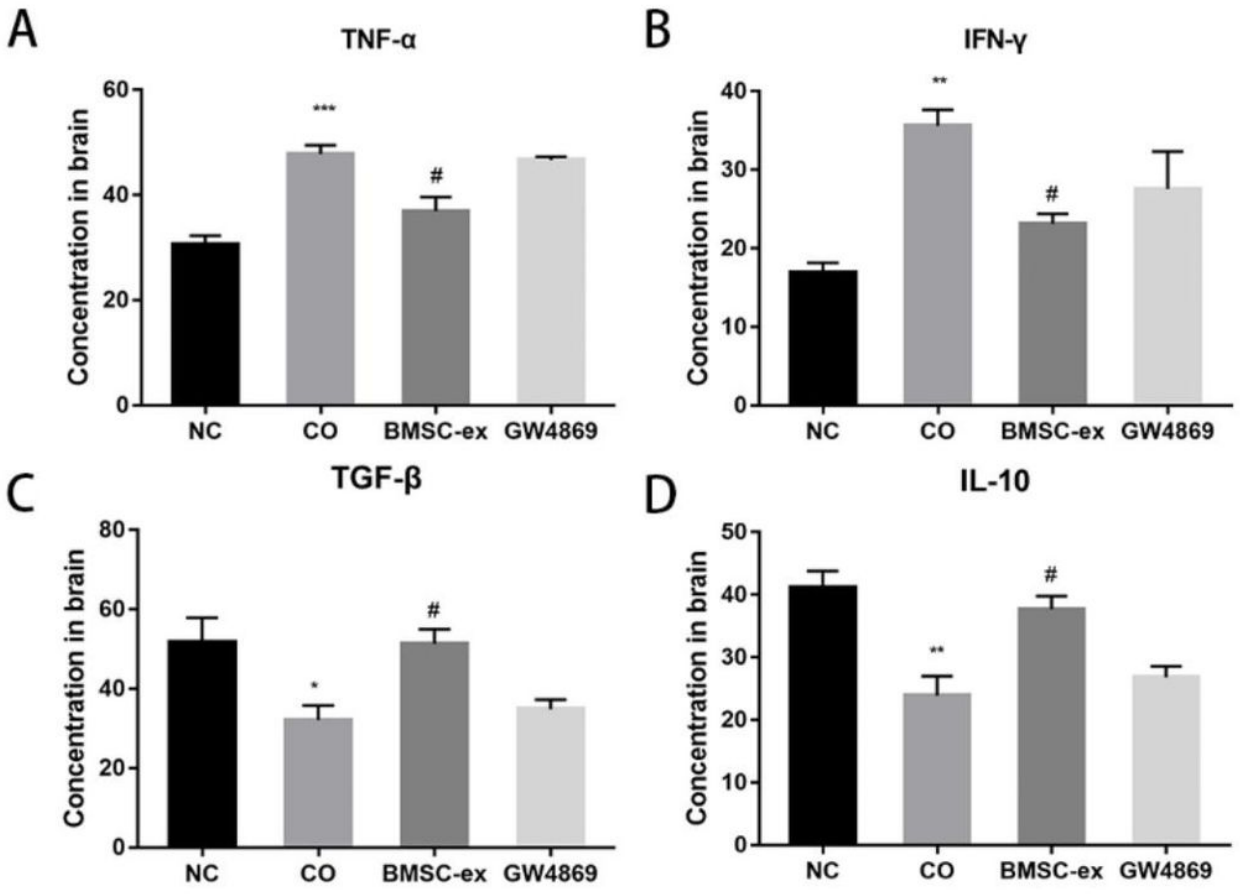

Figure 4

(A-D), The concentration of TNF-α, IFN-γ, TGF-β and IL-10 in brain tissues of mice by ELISA 14 days after CO exposure. (* P < .05, **P < .01, ***P < .001, ****P < 0.0001 vs.NC group; #P < 0.05, vs.CO group).

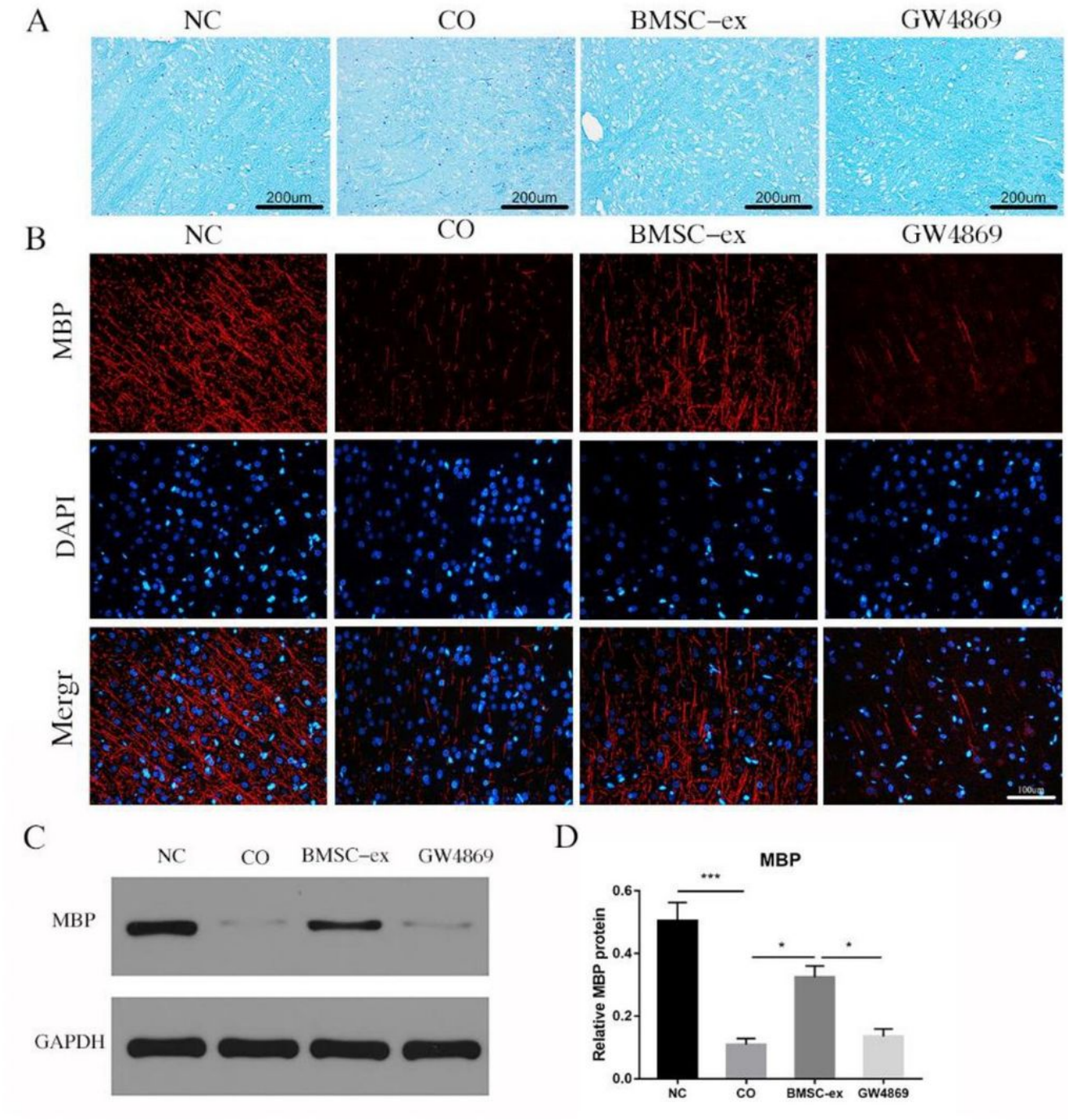

Figure 5

BMSC-derived exosomes promoted myelination and alleviated myelin sheath damage. (A) LFB staining images. (B)Immunofluorescence images showed the expression of MBP and nuclear in the NC, CO, BMSC-ex, BMSC-ex+GW4869 groups. (C) Western Blot and (D) quantification was utilized for detecting relative expression of MBP. The full-length blots gels images are presented in Supplementary FigureS2. (* P < .05, **P < .01, ***P < .001, ****P < 0.0001 vs.NC group; #P < 0.05, vs.CO group)

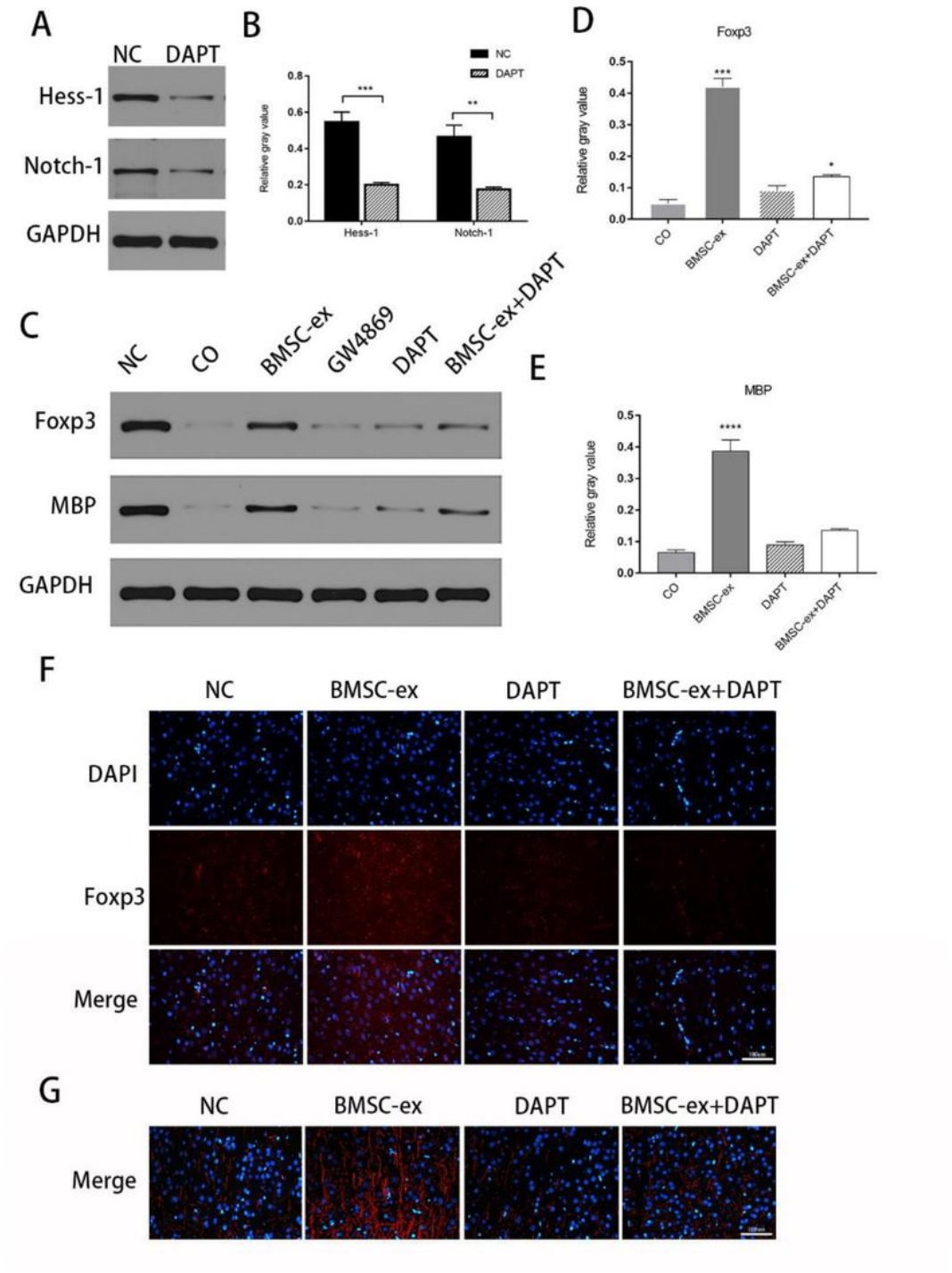

Figure 6

DAPT partly reversed the effect of BMSC-derived exosomes. (A) Western Blot and (B) quantifications were implemented for relative expression of Hess-1, Notch1 and GAPDH. The full-length blots gels images are presented in Supplementary FigureS3. (C) Western Blot and (D) quantifications were performed for the sake of relative protein expression for Foxp3, MBP and GAPDH. The full-length blots gels images are presented in Supplementary FigureS2. (F), Immunofluorescence images was used to show expression of

Foxp3 in the CO, BMSC-ex, DAPT, BMSC-ex+ DAPT groups. (G) Immunofluorescence images showing the expression of MBP in the CO, BMSC-ex, DAPT, BMSC-ex+ DAPT groups. (* P < .05, **P < .01, ***P < .001)

Supplementary Files

This is a list of supplementary files associated with this preprint. Click to download.

- supplementary.docx